

Y. Okaue, T. Yokoyama and T. Sakudo

Department of Chemistry, Faculty of Sciences, Kyushu University

**INTRODUCTION:** Silsesquioxanes used in this study are members of the cage-shaped oligosilsesquioxanes with cubic framework called double four-ring (D4R) structure as illustrated in Fig. 1. Upon  $^{60}\text{Co}$   $\gamma$ -ray irradiation at room temperature on trimethylsilylated silsesquioxane,  $\text{Q}_8\text{M}_8$  ( $[(\text{CH}_3)_3\text{SiO}]_8(\text{SiO}_{1.5})_8$ ), a stable hydrogen atom is encapsulated in the D4R cage. The encapsulation and stabilization of a hydrogen atom in the D4R cage were confirmed by ESR spectroscopy. ESR parameters and saturation behavior of signals for the encapsulated hydrogen atom in the D4R cage were influenced by paramagnetic oxygen molecules outside the cage without chemical attack.[1] The purpose of this study was to examine the encapsulation of a hydrogen atom in the D4R cage with some different substituents instead of trimethylsilyloxy group at each vertex of  $\text{Q}_8\text{M}_8$  as shown in Fig. 1.

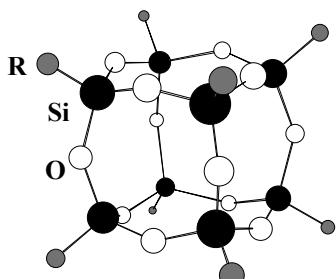
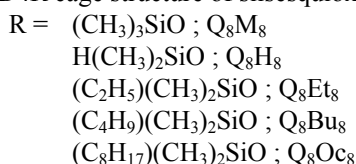


Fig. 1. D4R cage structure of silsesquioxane.



**EXPERIMENTS:**  $\text{Q}_8\text{M}_8$  was prepared by trimethylsilylation of octameric tetramethylammonium silicate (TMAS;  $[(\text{CH}_3)_4\text{N}]_8(\text{SiO}_{1.5})_8$ ). The other octasilsesquioxanes with D4R structure were synthesized by similar silylation methods on the basis of trimethylsilylation techniques. These silsesquioxanes were purified by recrystallization from hexane or separation with HPLC. After  $^{60}\text{Co}$   $\gamma$ -ray irradiation under air at room temperature, ESR spectra were measured at room temperature to examine the characteristics of the hydrogen atom encapsulated in the D4R cage of the five silsesquioxanes.

**RESULTS:** The pure  $\text{Q}_8\text{Bu}_8$  and  $\text{Q}_8\text{Oc}_8$  were obtained as gluey liquid at ambient temperature and pressure.

The other silsesquioxanes were obtained as white solid. After  $\gamma$ -ray irradiation of each silsesquioxanes, ESR spectrum at room temperature showed characteristic two hyperfine lines separated with 50.8 mT due to hydrogen atom encapsulated in the D4R cage as shown in Fig. 2.

Fig. 2 ESR spectrum of the hydrogen atom encapsulated in the D4R cage after  $\gamma$ -ray irradiation.

Encapsulation behaviors, such as encapsulation ratio, of the hydrogen atom in the D4R cage of the five silsesquioxanes were different depending upon the side chain substituents. As listed in Table, Zeeman splitting factor ( $g$ -value) and hyperfine splitting constant ( $A$ -value) for encapsulated hydrogen atom were approximately same among the five silsesquioxanes at room temperature. On the other hand, line width ( $\Delta H_{pp}$ ) of the signal due to the hydrogen atom encapsulated in liquid  $\text{Q}_8\text{Bu}_8$  or  $\text{Q}_8\text{Oc}_8$  was lower than those of other solid silsesquioxanes, especially, *in vacuo* ( $< 10^{-5}$  Torr).

Table ESR Parameters of Encapsulated Hydrogen Atom in Silsesquioxanes at Room Temperature

Silsesquioxane	$g$ -value	$A$ -value / MHz	$\Delta H_{pp}$ / mT
$\text{Q}_8\text{M}_8$ (in air)	2.0027	1415.2	0.10
$\text{Q}_8\text{M}_8$ ( $< 10^{-5}$ Torr)	2.0027	1415.7	0.10
$\text{Q}_8\text{H}_8$ (in air)	2.0027	1415.7	0.10
$\text{Q}_8\text{H}_8$ ( $< 10^{-5}$ Torr)	2.0028	1415.2	0.10
$\text{Q}_8\text{Et}_8$ (in air)	2.0027	1415.6	0.10
$\text{Q}_8\text{Et}_8$ ( $< 10^{-5}$ Torr)	2.0026	1415.7	0.10
$\text{Q}_8\text{Bu}_8$ (in air)	2.0027	1415.6	0.05
$\text{Q}_8\text{Bu}_8$ ( $< 10^{-5}$ Torr)	2.0027	1415.3	0.01
$\text{Q}_8\text{Oc}_8$ (in air)	2.0027	1415.2	0.07
$\text{Q}_8\text{Oc}_8$ ( $< 10^{-5}$ Torr)	2.0027	1415.3	0.01

In the cases of  $\text{Q}_8\text{Bu}_8$  and  $\text{Q}_8\text{Oc}_8$ , these hydrogen hyperfine transitions were further split by superhyperfine (shf) interactions with  $^{29}\text{Si}$  nuclei. These shf lines were observed as shoulders.

**REFERENCE:**

[1] R. Sasamori, Y. Okaue, T. Isobe, Y. Matsuda, Science, **265** (1994) 1691-1694.

T. Awano and T. Takahashi<sup>1</sup>

Department of Electronic Engineering, Tohoku Gakuin University

<sup>1</sup>Research Reactor Institute, Kyoto University

**INTRODUCTION:** Movement of ions is not in phase and frequent scattering by other mobile ions seems to decrease the ionic conductivity. If coherent excitation of ionic movement by coherent external electric field occurs, ionic conductivity seems to increase drastically. We have investigated sub-millimeter and far-infrared spectroscopy of superionic conductors to find such a correlative movement of conduction ion. Broad peak was observed at sub-millimeter region of energy loss function spectra of  $MA_4X_5$  ( $M=Rb, K, NH_4$ ;  $A=Ag$  or  $Cu$ ;  $X=I$  or  $Cl$ ) crystals. This peak was able to be considered as that by "ionic plasmon".

Coherent THz wave from LINAC of KURRI is so strong that the excitation effect is expected to be observed. If this excitation occurs, absorption spectrum in this region should change. The coherent THz wave is extremely strong so that precise absorption measurement of thick sample is possible. We have measured millimeter wave absorption spectra of silver halides - silver phosphate glasses to investigate the existence of such a collective movement of conduction ion.

**EXPERIMENTS:** Each content of AgI, AgBr, BiBr<sub>3</sub>, AgNO<sub>3</sub> and NH<sub>4</sub>H<sub>2</sub>PO<sub>4</sub> were melt at 600 C for 3 h. Then the melt was quenched between two copper blocks. Sample diameter was 20 mm and thicknesses were around 400  $\mu$ m and 800  $\mu$ m. Pairs of transmittances of thin and thick plates were measured to obtain absorption coefficient. Transmittance spectra of coherent millimeter wave were measured by a Martin-Puplett type interferometer. Sample absorption at high energy end was strong due to phonon absorption shoulder and ambiguity was large.

**RESULTS:** Figure 1 shows absorption spectra of  $(AgI)_{0.5}(AgPO_3)_{0.5}$  glass for millimeter wave of different intensities. As previously reported[1], two absorption bands were observed at 8.4 and 6.3  $cm^{-1}$ . Fig. 1 shows that the absorption intensity of the 8.4  $cm^{-1}$  band depends on the excitation intensity. This suggests that the 8.4  $cm^{-1}$  band is due to a sort of collective movement of conduction ions. The absorption intensity seems to depend on the logarithm of excitation intensity. Study on the detail of the mechanism of this absorption is underway.

Figure 2 shows increment absorption spectra of  $(BiBr_3)_{0.05}(AgPO_3)_{0.95}$  glass from absorption spectrum at 77K. Two absorption bands were observed at 8.5 and 6.1  $cm^{-1}$ . These positions of absorption bands are almost the same as those in  $(AgBr)_{0.4}(AgPO_3)_{0.6}$  glass (8.7 and 6.1  $cm^{-1}$ ) and slightly different with those in

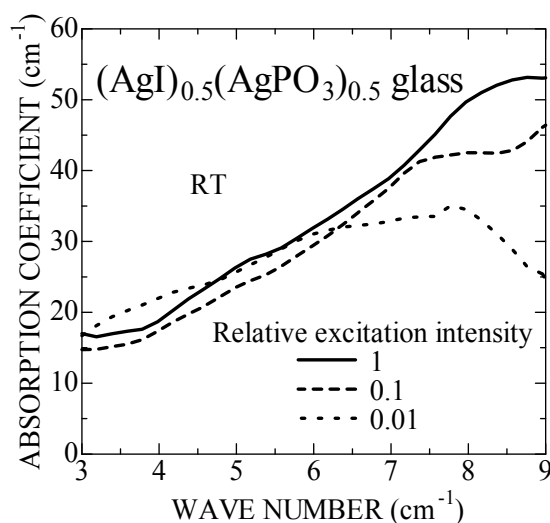


Fig. 1. Excitation intensity dependence of absorption spectra of  $(AgI)_{0.5}(AgPO_3)_{0.5}$  glass.

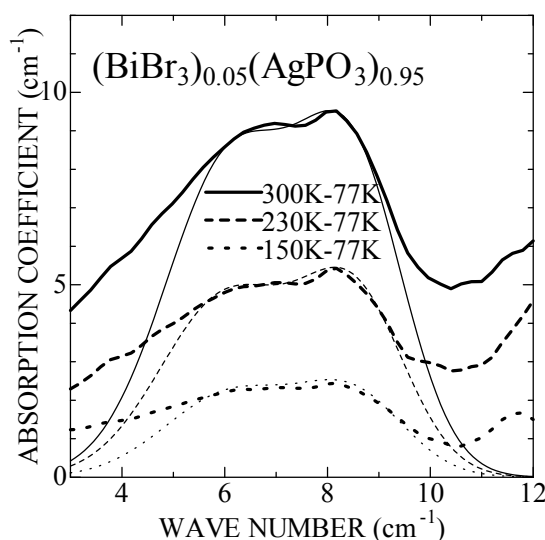


Fig. 2. Increment absorption spectra of  $(BiBr_3)_{0.05}(AgPO_3)_{0.95}$  glass from that at 77K. Thin lines show the summation of two Gaussian curves at 8.5 and 6.1  $cm^{-1}$  for each temperature.

$(AgI)_{0.5}(AgPO_3)_{0.5}$ . This means that these bands are related mainly with conducting silver ion and slightly with halogen ion.

**REFERENCE:**

[1] T. Awano and T. Takahashi, Journal of Physics: Conference Series, **148** (2009) 012040.

## CO4-3 Low Frequency Excitation in Maleic Acid Disodium/Acrylamide Gel

K. Hara, K. Terayama, N. Ueno, S. Yoshioka, M. Sugiyama<sup>1</sup> and T. Fukunaga<sup>1</sup>

Research Institute of Environment for Sustainability,  
Faculty of Engineering, Kyushu University

<sup>1</sup>Research Reactor Institute, Kyoto University

**INTRODUCTION:** Gels show unique characters by the interaction between two ingredients: solvent (water in case of hydrogels) and polymer network. Therefore, the authors have been studying their features, especially focusing on the effect of the solvent loss, namely, dehydration. As are expected, some hydrogels were found to show considerable property changes [1-3] in the investigations. Among them, one of the most noteworthy features related to the present study is the distinct low-frequency peak emergence in the Raman scattering spectrum of PAAm gel by dehydration [2], which demonstrates the emergence of some low energy excitation in the dehydrated PAAm gel. Besides, though the low-frequency Raman peak seems similar to the Boson peak which is well-known to exist in many of the glass materials, the temperature dependence of the Raman peak in the dehydrated gel was found to be different from that of the Boson peak by another authors' study [3]. This feature indicates the origin of the low-lying Raman peak in the hydrogel can be different from that of the Boson peak. Under these circumstances, the authors have further investigated the composition difference effect on the low-lying Raman peak in the dehydrated maleic acid disodium/acrylamide (MADS/AAm) gel in the present study.

**EXPERIMENTS AND RESULTS:** The low-frequency Raman spectra were observed by a micro-Raman spectroscopy (JASCO NRS-2100) installed at Kyoto University Research Reactor Institute. A He-Ne laser ( $\lambda=632.8\text{nm}$ ) was utilized as a source in order to avoid strong fluorescence from the sample. In addition, the pseudo-backscattering geometry was adopted to remove the natural emission from the Raman spectrum. Pre-gel aqueous solutions of the MADS/AAm gels with the total concentration of 700mM were prepared by dissolving maleic acid disodium salt hydrate and acrylamide with different ratios (2 : 5, 3 : 4). By adding 0.20wt% of *N,N'*-methylenebisacrylamide to the aqueous solution, the gelation was initiated; which was conducted by keeping the temperature at 60°C for 24hrs. After the gelation process, the gels were dehydrated at room temperature up to the water content of ~3.0%.

With these preparations, we observed the low frequency Raman spectrum of the dehydrated MADS/AAm gels and, as shown in Fig.1, they have found a spectral change in the low frequency region below 50 $\text{cm}^{-1}$  indicating that the functional group effect to the low-energy excitation. More detailed investigations are in preparation.

### REFERENCES:

- [1] T. Masuike *et al.*, Jpn. J. Appl. Phys. 1, **34** (1995) 4997-5000.
- [2] K. Hara *et al.*, Jpn. J. Appl. Phys. 1, **34** (1995) 5700-5705.
- [3] K. Hara *et al.*, Jpn. J. Appl. Phys. 2, **36** (1997) L1182-L1184.

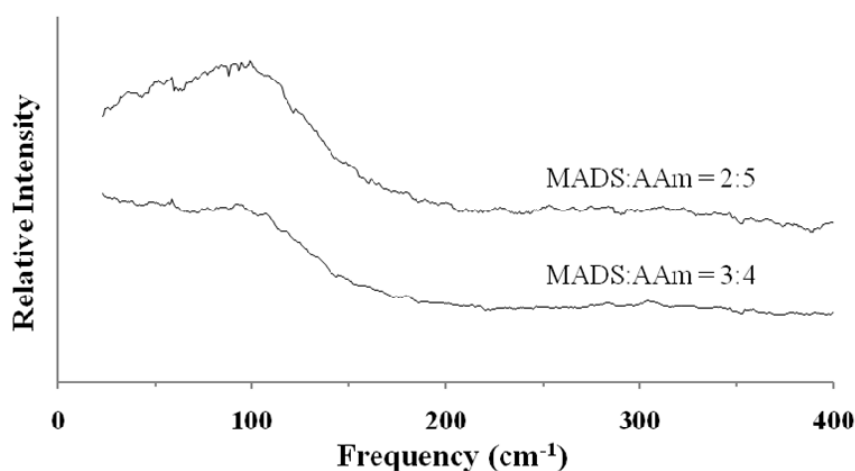


Fig. 1. The low frequency Raman spectra of the dehydrated MADS/AAm (MADS:AAm =2:5 and 3:4) gels.

## CO4-4 Study on Annihilation Behavior of Defects Produced in $\gamma$ -ray-irradiated $\text{Li}_2\text{TiO}_3$

K. Okuno, Y. Oya, A. Yoshikawa, H. Ishikawa, Y. Kikuchi, S. Suzuki, H. Yamana<sup>1</sup> and O. Shirai<sup>1</sup>

Radioscience Research Laboratory, Faculty of Science, Shizuoka University

<sup>1</sup>Research Reactor Institute, Kyoto University

**INTRODUCTION:** Several studies have been carried out over years to establish a tritium recovery system. Especially, lithium titanate ( $\text{Li}_2\text{TiO}_3$ ) is thought to be one of the candidates as the tritium breeding material on ITER. Our group has been reported that tritium release from neutron-irradiated  $\text{Li}_2\text{TiO}_3$  correlated with the annihilation of  $\text{E}'$ -center which was an oxygen vacancy occupied by one electron<sup>[1]</sup>. Therefore, elucidation of behavior of irradiation defects is an important issue to establish the tritium recovery system.

In this study, our attention was paid to the correlation between the produce and annihilation processes of the irradiation defects. The  $\gamma$ -ray irradiation which was different from neutron irradiation on the produce processes of the irradiation defects, was performed. Measurements of Electron Spin Resonance (ESR) were employed to follow the irradiation defects which were produced with various irradiation doses. Additionally, the annihilation behaviors of the each sample were evaluated by the isochronal annealing experiments.

**EXPERIMENTS:** The samples of  $\text{Li}_2\text{TiO}_3$  were irradiated by  $\gamma$ -rays (dose rate:  $3.24 \text{ kGy h}^{-1}$ , temperature: R.T.) with irradiation dose up to 300 kGy using  $^{60}\text{Co}$  irradiation setup in the Research Reactor Institute, Kyoto University (KURRI). After  $\gamma$ -ray irradiation, ESR (JEOL, JES-TE200) measurements were performed at liquid nitrogen temperature at the Center for Instrumental Analysis, Shizuoka University. Isochronal annealing experiments were performed to investigate the annihilation processes of irradiation defects. The annealing experiments were carried out until the ESR signals were either too small to detect or showed little further change.

**RESULTS:** The ESR spectrum of  $\gamma$ -ray-irradiated  $\text{Li}_2\text{TiO}_3$  consisted of three major peaks, namely,  $\text{O}^-$ -center, which was an oxygen hole center,  $\text{E}'$ -center and metallic lithium (Li) colloid<sup>[2]</sup>. Here,  $\text{O}^-$ -center and  $\text{E}'$ -center are a Frenkel pair. It was found that Li colloids increased as the irradiation dose increased up to 150 kGy, whereas the amounts of  $\text{O}^-$ -center and  $\text{E}'$ -center were decreased. On the other hand, the concentration of Li

colloids decreased in further irradiation dose, however those of  $\text{O}^-$ -center and  $\text{E}'$ -center were increased. It was considered that the decomposition of the Li colloids by  $\gamma$ -ray irradiation above 150 kGy lead to the increasing of the amounts of  $\text{O}^-$ -center and  $\text{E}'$ -center. This fact suggested that the existence of Li colloids affected the formation of  $\text{O}^-$ -center and  $\text{E}'$ -center. Figure 1 shows the annihilation behavior of the irradiation defects in isochronal annealing on the  $\gamma$ -ray-irradiated sample with 300 kGy. From these results, it was found that the annihilation of  $\text{O}^-$ -center and  $\text{E}'$ -center around 500-700 K were complementary. Taking this result into consideration, these defects would be recombined. According to the results of isochronal annealing experiments on each  $\gamma$ -ray irradiated sample, the changes of the annihilation behaviors of  $\text{O}^-$ -center and  $\text{E}'$ -center have a correlation with irradiation dose. It was suggested that Li colloids affected the annihilation of  $\text{O}^-$ -center and  $\text{E}'$ -center. From this study,  $\text{O}^-$ -center and  $\text{E}'$ -center, which produced by the  $\gamma$ -ray irradiation, were simultaneously annihilated by a recombination process, suggesting that this recombination process was affected by Li colloids. In future work, an influence of Li colloids on the annihilation of  $\text{O}^-$ -center and  $\text{E}'$ -center will be elucidated.

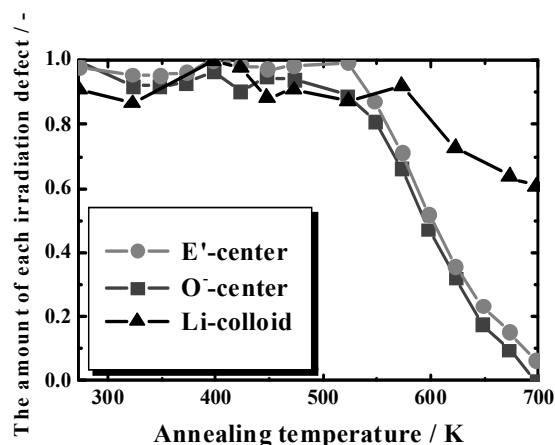


Fig. 1. Annihilation behavior of the irradiation defects in isochronal annealing experiments (300 kGy)

### REFERENCES:

- [1] K. Okuno and H. Kudo, *J. Nucl. Mater.*, **138** (1986) 31-35.
- [2] T. Teshima, *et al.*, *J. Appl. Phys.* **41** (2002) 685.

S. Okuda, T. Kojima, R. Taniguchi, S. Sakamoto and T. Takahashi<sup>1</sup>

Radiation Research Center, Osaka Prefecture University  
<sup>1</sup>Research Reactor Institute, Kyoto University

**INTRODUCTION:** Coherent synchrotron and transition radiation from electron bunches of a linear accelerator (linac) has a continuous spectrum at relatively high peak-intensity in a submillimeter to millimeter wavelength range, which approximately corresponds to a THz frequency range. Coherent radiation light sources for spectroscopic applications were first established in Kyoto University and Osaka University [1, 2].

Recently, the absorption spectroscopy system using the coherent transition radiation from the electron beams of the L-band electron linac under relatively simple configurations has been established at KURRI [3]. With this system absorption spectroscopy has been carried out for various kinds of samples in the present work. The results for the liquid sample, Poly (vinyl alcohol) (PVA) aqueous solution, which has relatively strong light absorbance, are reported. The irradiation effect of PVA with gamma rays have also been investigated.

**EXPERIMENTAL METHOD:** The electron beams of the 46 MeV KURRI L-band linac were used for experiments. The macropulse lengths of the beam were from 10 ns to 4  $\mu$ s. Coherent transition radiation was emitted from an aluminum foil. The configurations for the absorption spectroscopy are schematically shown in Fig. 1. Output light from a Martin-Puplett type interferometer, linearly polarized, was focused at a light collimator with 8 mm  $\phi$  diameter located just before a sample. The light path was in the air atmosphere. The detector was a liquid-He-cooled silicon bolometer.

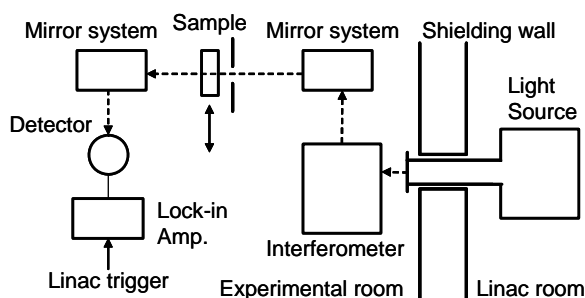


Fig. 1. Schematic diagram of the configurations for the absorption spectroscopy.

The wavenumber resolution was 0.1  $\text{cm}^{-1}$ . It took about 10 minutes in a measurement. The light spectrum was obtained by averaging over three or four measurements. The spectrum was considerably stable during the meas-

urements within  $\pm 2$ -3% in a wavenumber range of 4-13  $\text{cm}^{-1}$ . The details of the light source are described in ref. 3.

Irradiation of the sample with Co-60 gamma rays was carried out by using the facility at KURRI. The absorbed dose rate for irradiation was 11 kGy/h.

**ABSORPTION SPECTROSCOPY FOR PVA AQUEOUS SOLUTION:** Aqueous solution of 5 wt% PVA 0.08 mm thick was sandwiched with quartz plates 3 mm thick. Figure 2 shows the wavenumber dependence of the transmittance of light obtained for the sample before and after the gamma-ray irradiation at a total absorbed dose of 50 kGy. The periodic oscillation observed on the spectrum can be attributed to the interference between lights transmitting through the sample and those reflected at the surfaces of the quartz plates. From the results for the present work it was found that the transmittance of light increased with irradiation dose at doses below 50 kGy and decreased above the dose to be almost the same transmittance at a dose of 70 kGy, at which the formation of PVA gels was observed. This suggests the light transmittance is closely related to the gel formation determining the behaviors of water molecules.

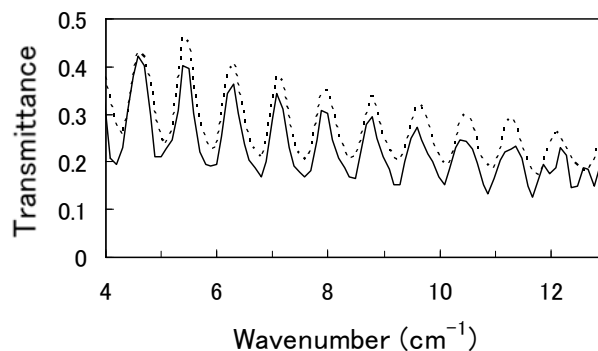


Fig. 2. Wavenumber dependence of light transmittance for PVA aqueous solution 0.08 mm thick sandwiched with quartz plates 3 mm thick, before (solid line) and after (dotted line) the irradiation with gamma rays at an absorbed dose of 50 kGy.

For some of the other samples the effects of the intensity of the coherent radiation has been observed. The main purpose of the researches in the future will be the investigation of these effects.

#### REFERENCES:

- [1] T. Takahashi, T. Matsuyama, K. Kobayashi, Y. Fujita, Y. Shibata, K. Ishi and M. Ikezawa, Rev. Sci. Instrum. **69** (1998) 3770.
- [2] S. Okuda, M. Nakamura, K. Yokoyama, R. Kato and T. Takahashi, Nucl. Instrum. Meth. **A445** (2000) 267.
- [3] S. Okuda and T. Takahashi, Infrared Phys. Technol. **51** (2008) 410.

T. Takahashi

Research Reactor Institute, Kyoto University

**INTRODUCTION:** For the spectroscopic purpose, various types of coherent radiation emitted from a relativistic electron beam have attracted a considerable attention as a new and powerful light source in the THz-wave region. Coherent transition radiation (CTR) is one of such a light source. Whereas synchrotron radiation has linear polarization along an electron orbit, the electric vector of transition radiation (TR) emitted from a metallic screen is axially symmetric with respect to the trajectory of an electron beam. Therefore, CTR is usually utilized as a non-polarized light source in the spectroscopic application. However, circularly polarized light has been useful in the circular dichroism spectroscopy. Shibata *et al.* has developed a technique of generation of circularly polarized THz-wave radiation with the phase difference between the forward TR and the backward TR [1]. However, it was difficult to control the polarization degree because the geometrical arrangement was important in order to generate both the linearly polarized the forward and the backward TR. In this report the new technique of generation of linearly polarized CTR with a radiator of a wire grid.

**EXPERIMENTAL PROCEDURES:** The experiment was performed at the coherent radiation beamline [2] at the 40-MeV L-band linac of the Research Reactor Institute, Kyoto University. The width of the macro pulse and the repetition rate of the electron beam were 47 ns and 46 Hz, respectively. The average current of the electron beam was 1.8  $\mu$ A. The schematic layout of the experiment is shown in Fig. 1. As the radiator (R in Fig. 1) of backward CTR a flat aluminum foil 15  $\mu$ m thick and a wire grid 10  $\mu$ m thick with 25mm spacing were used. The direction of the wire grid was vertical. This radiator also reflected the forward CTR emitted from a titanium window. The superposition of two kinds of CTR was detected by a liquid-helium-cooled Si bolometer. In order to measure the polarization a wire-grid polarizer was used in front of the detector.

**RESULTS:** The intensity variation as a function of the azimuth angle of the polarization was observed by rotating the wire-grid polarizer. The observed intensity with the aluminum foil radiator is shown by the dashed curve in Fig. 2. Zero degree corresponds to the vertical component of radiation. Though CTR from a metallic foil has non-polarization, the dashed curve in Fig. 2 shows

the weak variation. The reason arises from the slight discrepancy between the electron trajectory and the optical axis. With a wire grid as a radiator the observed intensity variation is shown by the solid curve in Fig. 2. It clearly represents that the observed radiation has a vertical polarization. The linearly polarized CTR with a wire-grid radiator was first observed and this technique has proved useful for generation of circular polarized CTR with controlling the phase difference between the linearly polarized forward CTR and the backward one. This result will lead to the development of the high-resolution time-resolved circular dichroism spectroscopy in the THz-wave region.

#### REFERENCES:

- [1] Y. Shibata *et al.*, Rev. Sci. Instrum. **72** (2001) 3221.
- [2] T. Takahashi *et al.*, Rev. Sci. Instrum. **69** (1998) 3770.

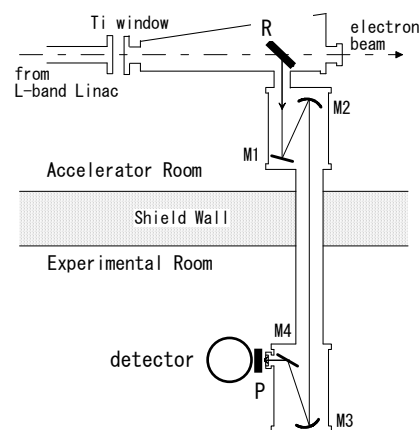


Fig.1. The arrangement of the experiment. Keys are: (R) a radiator of backward CTR, (M1, M4) flat mirrors, (M2, M3) spherical mirrors, (P) a polarizer.

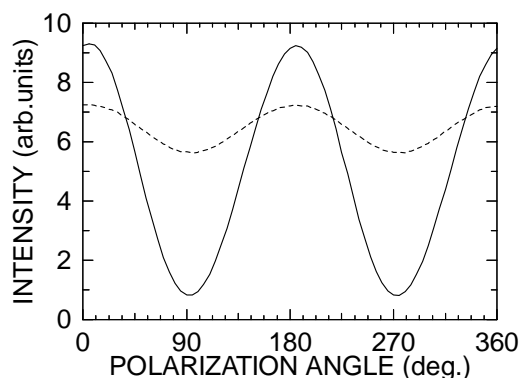


Fig.2. Intensity variation of CTR with a wire-grid (solid curve) and an aluminum foil (dashed curve) as a radiator.

## CO4-7 Complex Structure of Ions Coordinated with Hydrophilic Polymer. 9:

A. Kawaguchi, Y. Gotoh<sup>1</sup> and Y. Morimoto

Research Reactor Institute, Kyoto University  
<sup>1</sup>Faculty of Text. Sci. and Tech., Shinshu Univ.

**INTRODUCTION:** We have reported *in situ* hybrid composite structure through "secondary doping" by diffusion of metallic ions into the iodinated hydrophilic polymers; in a case of silver ion, Ag<sup>+</sup>, as the "secondarily doped ion", organic-inorganic composite structures are prepared as precipitation of AgI salt and other hybrid coordination proceeds at inner space of the hydrophilic polymer.[1,2] Procedures suggested here achieves novel complex structures without synthesis, nor melting, nor casting, nor blending through various stages of the composite, and even metallization is realizable; for example, (at least) three kinds of stages exist in the "Ag<sup>+</sup>/I<sub>n</sub><sup>-</sup>/PA6" hybrid composite: "stage I / II / III".[2,3] Furthermore, qualitative similarity is found for other matrix of hydrophilic polymers, such as PVA or regenerated cellulose.[4] Such singularity and diversity and similarity are attributed to existence of polyiodide ions, I<sub>n</sub><sup>-</sup> (n = 3,5,...), which are previously doped in the polymeric structure. Under such environment of "inner volume" of polymers, ions can be diffused with influence of polymer chain; hydrophilic or functional groups on the chain can be regarded both as restricting coordination sites and as medium for diffusion.[5-7]

**EXPERIMENTS:** As starting samples of non-doped PA6 (polyamide-6, Nylon<sup>TM</sup>-6), commercial films ("Rayfan #1401" in thickness of 0.1mm, Toray Film co.ltd.) were used. The cut pieces of filmy sample were immersed within an I<sub>2</sub>-KI aqueous solution (0.2-0.8N) to prepare "PA6/polyiodide complex"; this procedure is called as "(first) iodine doping".[6-8] After drying, the iodinated PA6 was immersed in a AgNO<sub>3</sub> aqueous solution of 0.2-1.0M. ("secondary doping") Each doping process was terminated by rinsing the samples with distilled water. On the other hand, bulk AgI was prepared by filtration of precipitate after mixing AgNO<sub>3</sub>(aq) and KI(aq) solutions.

After preparation of each stage, "stage I / II / III", their cut pieces and bulk AgI salt were encapsulated in quartz capillaries and were investigated with Raman spectroscopy by Ar laser. (JASCO NR-1100)

**RESULTS AND DISCUSSION:** Generally, iodine is coordinated in hydrophilic polymers as polyiodide ions, such as I<sub>3</sub><sup>-</sup>, I<sub>5</sub><sup>-</sup>, or more. And these polyiodide ions exist in different proportion from one in regular aqueous solution; for example; pentaiodide ion, I<sub>5</sub><sup>-</sup>, plays dominant roles as dopants coordinated in the iodinated polymers while it is regularly a minor components in aqueous solution. [7-9]

In Raman spectroscopy, polyiodide ions doped in PA6 matrix are identified as I<sub>3</sub><sup>-</sup> and I<sub>5</sub><sup>-</sup>, which show peaks of 115cm<sup>-1</sup> (for I<sub>3</sub><sup>-</sup>) or 160-170cm<sup>-1</sup> (for I<sub>5</sub><sup>-</sup>).[8,9] On the other hand, "stage I / II / III" indicated other profiles.

(Fig.1) A profile given by AgI salt (bulk) precipitated in aqueous system is also compared in Fig.1. The results have to be estimated more precisely in future since the profiles indicated both difference between the stages and some unidentified peaks (75 or 117 cm<sup>-1</sup>, instrumental noise?) However, these results suggest that coordinated polyiodide ions in the iodinated polymers have been completely transformed into other stages in the organic-inorganic composite and that precipitated fillers in yellow "stage II" is different from one in both green "stage I" and colorless "stage III". So, we can conclude that specification of "stage I / II / III" is contributed by some diverse structures of fillers in the composite.

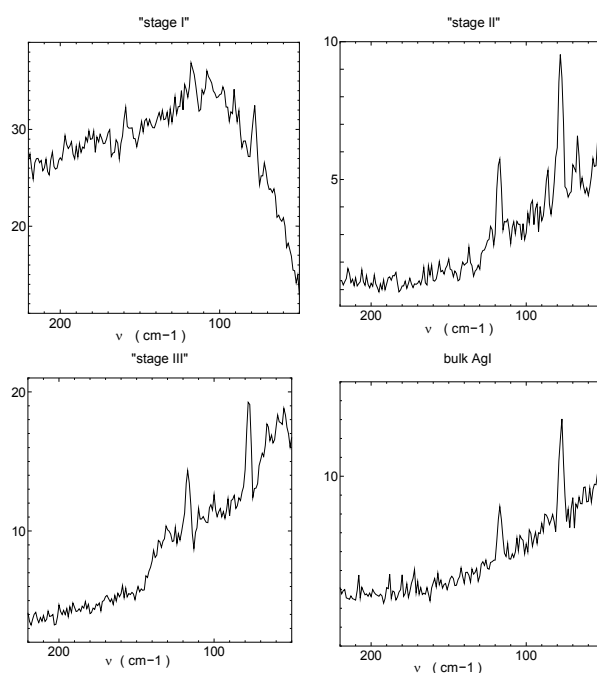


Fig. 1. Raman spectra for "stage I" (left, upper), "II" (right, upper), "III" (left, lower), bulk AgI (right, lower). (Peaks at 75 or 117cm<sup>-1</sup> may be noise?)

### REFERENCES:

- [1] A. Kawaguchi, *et. al.*, *Macromolecular Symposia*, **202** (2003) 77-83.
- [2] Y. Fujimori, *et. al.*, *J. Appl. Polym. Sci.*, **108** (2008) 2814-2824.
- [3] A. Kawaguchi, *et. al.*, *Polym. Prep. Jpn.*, **55** (2006) 1004-1004.
- [4] PAT. submitting, PCT/JP2007/051037.
- [5] A. Kawaguchi, *et. al.*, *KURRI Prog. Rep.* 2007, 197-197 (2008).
- [6] A. Kawaguchi, *et. al.*, *SPRING-8 User Experiment Rep.* **5** (2005B) (2006) (on-line).
- [7] A. Kawaguchi, *et. al.*, *Photon Factory Act. Rep.* 2007, **25** (2008) 113-113.
- [8] A. Kawaguchi, *Polymer*, **33** (1992) 3981-3984.
- [9] N.S. Murthy, *et. al.*, *J. Polym. Sci. Polym. Phys. Ed.*, **23** (1985) 2369-2376.

## CO4-8 Effect of Concentration of HNO<sub>3</sub> on Stability of Pyrrolidone Precipitants against $\gamma$ -Irradiation under Heating

M. Nogami, T. Kawasaki, Y. Sugiyama, M. Harada and Y. Ikeda

Research Laboratory for Nuclear Reactors, Tokyo Institute of Technology

**INTRODUCTION:** We have been developing a novel reprocessing system for spent FBR fuels based on the two precipitation processes[1]. In this system, pyrrolidone derivatives (NRPs) are used for the selective precipitation of U(VI) or both U(VI) and Pu(IV, VI). It is necessary to evaluate the stability of the precipitants for developing the system. In our previous studies on the stability for several NRPs, their applicability was confirmed by the precipitation abilities for U(VI) for the samples irradiated up to 70 kGy under heating at 50°C in 3 mol·dm<sup>-3</sup> (= M) HNO<sub>3</sub> solutions, where apparent decreases in the precipitation ratio for U(VI) were not observed[2]. In this study, similar examinations were performed by using 6 M HNO<sub>3</sub> solutions in order to investigate the effect of the concentration of HNO<sub>3</sub>.

**EXPERIMENTS:** The NRPs used were *N-n*-propyl-2-pyrrolidone (NproP), *N-n*-butyl-2-pyrrolidone (NBP), and *N-iso*-butyl-2-pyrrolidone (NiBP) as the precipitants with lower hydrophobicity and donicity, and *N*-(1,2-dimethyl)-propyl-2-pyrrolidone (NDMProP), *N*-neopentyl-2-pyrrolidone (NNpP), and *N*-cyclohexyl-2-pyrrolidone (NCP) as those with higher hydrophobicity and donicity, respectively.  $\gamma$ -irradiation under heating at 50°C was conducted by the similar manner as previously reported[2]. The reaction time was 43h in all cases and the dose rates varied depending on the NRP (4.8 to 8.2 kGy·h<sup>-1</sup>). Aliquots of the sample solution were taken at appropriate intervals and the precipitation ratio for U(VI) (P) was determined by contacting with 6M HNO<sub>3</sub> solutions containing 1M U(VI). The stability of the precipitant was evaluated by comparing the P values with the untreated one (P<sub>0</sub>) for each NRP.

**RESULTS:** A gas continues to generate from all of the 6 samples after the end of the irradiation. The changes in P/P<sub>0</sub> of NRPs versus treated time are shown in Fig. 1. It has been found that, unlike the cases for the 3M HNO<sub>3</sub> solutions, P/P<sub>0</sub> values for NProP, NBP, NNpP are decreased by the irradiation of less than 70 kGy. These results indicate that the degradation of NRPs by  $\gamma$ -irradiation under heating proceeds more easily in higher concentration of HNO<sub>3</sub>. While, NiBP and NDMProP have shown more stable properties because the P/P<sub>0</sub> values were found to be almost constant. The difference in the stability of NRPs would be explained by the branching property of *N*-substituted alkyl group. Namely, the stability of those substituted by a straight-chain is weaker.

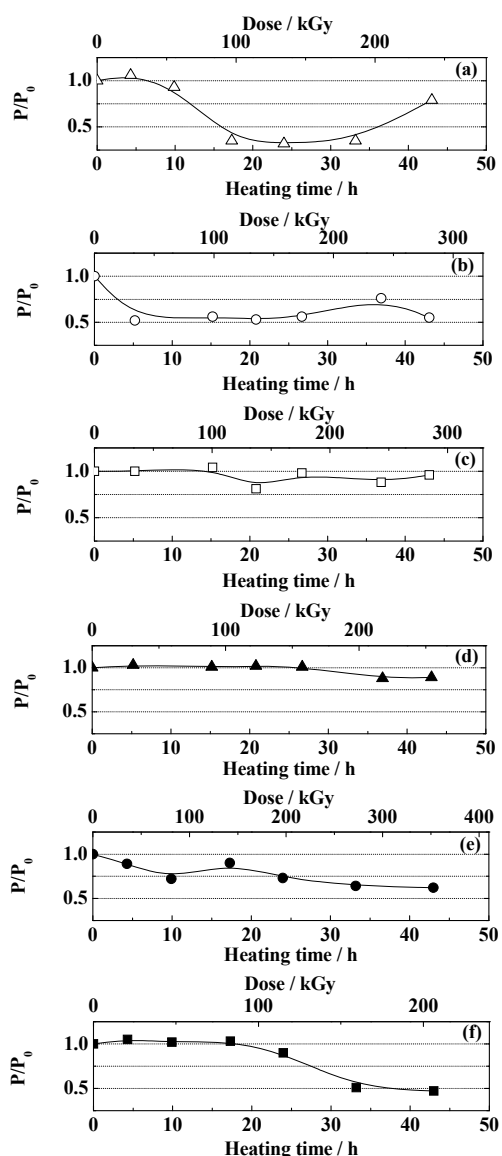


Fig. 1. Change in P/P<sub>0</sub> of NRPs treated in 6M HNO<sub>3</sub> as a function of time; (a) NProP, (b) NBP, (c) NiBP, (d) NDMProP, (e) NNpP, (f) NCP.

**ACKNOWLEDGMENT:** Present study is the result of “Development of Advanced Reprocessing System Using High Selective and Controllable Precipitants” entrusted to Tokyo Institute of Technology by the Ministry of Education, Culture, Sports, Science and Technology of Japan (MEXT).

### REFERENCES:

- [1] Y. Ikeda, *et al.*, Proc. Intl. Conf. on Advanced Nuclear Fuel Cycles and Systems (GLOBAL2007), (2007) 1503-1507.
- [2] M. Nogami, *et al.*, KURRI Prog. Rep. **2007**, (2008) 201.



## CO4-9 Effects of UV Irradiation on ESR and Optical Properties of Cu(II) Ions in Organic Solid Solutions Containing CuCl at 77 K

Y. M. Hase, Y. Nakano<sup>1</sup> and T. Saito<sup>1</sup>

Faculty of Engineering Science, Osaka University

<sup>1</sup>Research Reactor Institute, Kyoto University

**INTRODUCTION:** Effects of the structural changes due to ligand atoms on the electrical redox potential of Cu(I)/Cu(II) have been studied by investigating the effects of uv irradiation on ESR and Optical properties of Cu(II) ions in organic solid solutions containing CuCl at 77 K<sup>1</sup>. We have been investigating the ESR and optical properties of Cu atom produced radiation-chemically by reducing their mono cations in solid solutions.<sup>2-4</sup> In order to obtain further information on the dynamical changes of the ligand structure around the central metal ions caused by uv and  $\gamma$  irradiation and to elucidate the formation mechanism and stabilization of exciplexes produced by uv and  $\gamma$  irradiation, the ESR and optical studies have been carried out for 2-methyltetrahydrofuran (MTHF) and ethanol (EtOH) solid solutions with HCl containing CuCl.

**EXPERIMENTS:** Reagent grade of CuCl was purchased and was used for preparing the solutions without further purification. Reagent grade MTHF was distilled fractionally. The UVB-lamp and the UVC-lamp (Philips TL12 and TUV; NIPPON P · I CO., LTD.) with the peak wavelength at 310 nm and 253.7 nm were used. All the uv and the  $\gamma$  irradiation were carried out at 77K. The ESR, optical absorption, emission and excitation measurements were carried out with use of JEOL at 73 K, MPS-5000L at 77 K and F-4500 at 77 K, respectively.

**RESULTS AND DISCUSSION:** The new ESR signals observed after uv irradiation at 73 K for the first time<sup>3</sup> is inferred to Cu(II) ions of a transformed ligand structure that is formed *via* an exciplex “adiabatically”. We infer that the new species induced by uv irradiation forms strong covalent bonds between Cu(II) ions and the ligand. The new absorption band at 400-500 nm together with the new emission band at 480 nm observed after uv irradiation corresponds to the new set of four ESR lines appeared after uv irradiation as shown in Fig. 1. Considering the results of ESR and optical properties together with the previous results, the emissive, excited species can be classified into three types. The optical properties of the solutions before and after uv irradiation obtained in this study have showed evidence for the formation of the new complex induced by uv irradiation. We propose that the species prior to uv irradiation has a square planer structure, while after uv irradiation it is transformed into a species that is twisted into a tetrahedral direction.

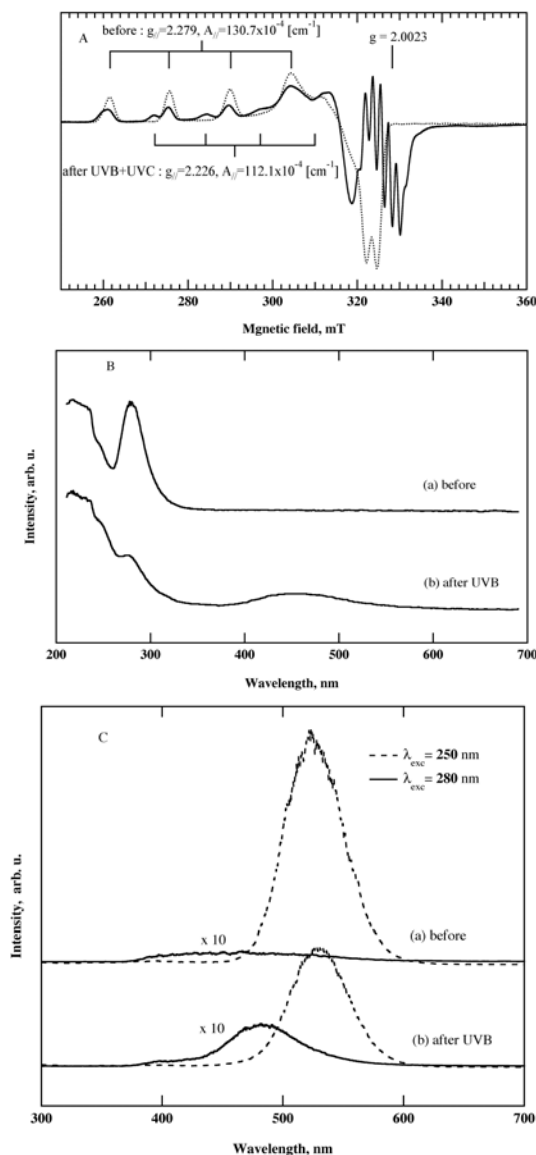


Fig. 1. ESR spectra (A) observed at 73 K, optical absorption spectra (B) and Emission spectra (C) observed at 77 K before and after uv irradiation for the solid solutions of MTHF containing  $10^{-1}$  M CuCl with 0.2 ml HCl per solvent of 10 ml, respectively. The total dose of uv irradiation was typically  $1.2 \text{ J/cm}^2$ .

### REFERENCES:

- [1] Y. M. Hase, Y. Nakano, T. Saito, *The Open Mag. Res. J.*, **1** (2008) 81-87.
- [2] Y. M. Hase, Y. Nakano, T. Saito, *Prog. Rep. KURRI* 2007, 191.
- [3] Y. M. Hase, Y. Nakano, T. Saito, *Prog. Rep. KURRI* 2006, 185.
- [4] Y. Miyatake, H. Hase, K. Matsuura, M. Taguchi, M. Hoshino, S. Arai, *J. Phys. Chem., B* **102** (1998) 8389-8394.

T. Takahashi, T. Iizuka<sup>1</sup> and S. Kimura<sup>2,1</sup>

Research Reactor Institute, Kyoto University

<sup>1</sup>School of Physical Sciences, The Graduate University for Advanced Studies

<sup>2</sup>UVSOR Facility, Institute for Molecular Science

**INTRODUCTION:** In recent years, various types of coherent radiation emitted from a relativistic electron beam have attracted a considerable attention as a new and powerful light source in the THz-wave region. The technique of near-field THz-wave microscopy is a characteristic application of such brilliant coherent radiation. This technique provides high spatial resolution below the diffraction limit. In the storage ring BESSY-II (Germany), spatial resolution power of  $\lambda/40$  was obtained at  $2\text{ cm}^{-1}$  using coherent synchrotron radiation [1]. In this report some basic properties, i.e. spatial resolution and spectrum, are experimentally investigated in the illumination mode in order to establish the technique of near-field microscopy with coherent transition radiation (CTR).

**EXPERIMENTAL PROCEDURES:** The experiment was performed at the coherent radiation beamline [2] at the 40-MeV L-band linac of the Research Reactor Institute, Kyoto University. The width of the macro pulse and the repetition rate of the electron beam were 47 ns and 46 Hz, respectively. The charge of a bunch was 1.2 nC. The THz-wave source was CTR emitted from an aluminum foil with 15- $\mu\text{m}$  thickness. The radiation was detected by a liquid-helium-cooled Si bolometer. The conical cone with an aperture 260  $\mu\text{m}$  in diameter was used as the illumination probe and its F-number was 2.5. The spectrum of CTR was measured by a Martin-Puplett type interferometer.

**RESULTS:** In order to investigate the spatial resolution, a stainless steel sheet with a hole 1 mm in diameter was scanned in front of the aperture on the top of the illumination probe. The observed intensity of the transmitted radiation through the hole is plotted in Fig. 1 and its first derivative is shown by a dotted curve in Fig. 2. The width of the derivative curve is equivalent to the spatial resolution. The resolution of 170  $\mu\text{m}$  was derived from the Gaussian fitting of the derivative curve in Fig. 2. In Figure 3, the solid and dashed curves show the observed CTR spectra through and without the illumination probe, respectively. The former intensity was multiplied by 1000 in this figure to clarify the difference

of the spectral shape from the latter. The shift of the spectral distribution to shorter wavelengths arises from passing through the aperture probe. Considering the wavelength of 750  $\mu\text{m}$  at peak intensity, the spatial resolution power was evaluated to be  $\lambda/4$ .

**ACKNOWLEDGMENTS:** This work was partly supported by Quantum Beam Technology Program of MEXT, Japan.

**REFERENCES:**

- [1] U. Shade, *et al.*, Appl. Phys. Lett., **84** (2004) 1422.  
 [2] T. Takahashi, *et al.*, Rev. Sci. Instrum., **69** (1998) 3770.

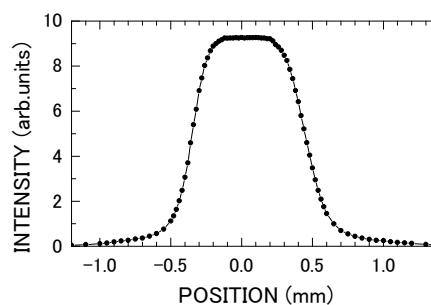


Fig. 1. Scanning curve of a hole of 1 mm in diameter using a near field probe.

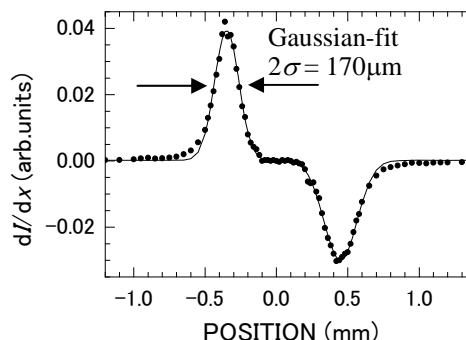


Fig. 2 First derivative curve of Fig. 1 (dotted line) and the Gaussian fitting (solid line).

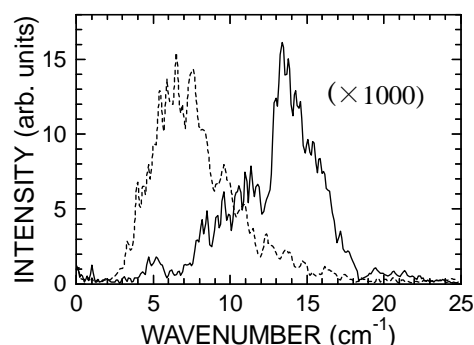


Fig. 3. Observed spectra of CTR with (solid) and without (dashed) the near-field probe.